Physica 112B (1982) 24–32
North-Holland Publishing Company

FLUX PENETRATION AND a.c. LOSSES IN TYPE II SUPERCONDUCTORS

II. EXPERIMENTS ON Nb–50% Ti

E.A. GIJSBERTSE, J.L. DE REUVER and L.J.M. VAN DE KLUNDERT

Twente University of Technology, Department of Applied Physics, P.O.B. 217, 7500 AE Enschede, The Netherlands

Received 3 August 1981

The a.c. behaviour of Nb–50% Ti can be described in terms of the quasi-static Critical State Model. The critical current density j_c as a function of position and magnetic induction as well as the $B_{en}(B_a)$ and $B_{ex}(B_a)$ relations which describe the surface screening currents have been determined experimentally with the help of trapezoidal a.c. fields. The results are in agreement with the calculated induced voltage waveforms presented in part I.

1. Introduction

The behaviour of type II superconductors is usually described in terms of the Critical State Model (C.S.M.) [1]. In this model two types of supercurrents can be distinguished: bulk currents described in terms of the critical current density j_c and surface currents which flow in a very narrow layer at the surface. In the irreversible case the latter may be described by $B_{en}(B_a)$ and $B_{ex}(B_a)$ in an increasing respectively decreasing external magnetic field B_a. A more detailed description of this quasi-static C.S.M. has been given elsewhere [2–4]. The influence of these parameters on measurable quantities such as induced voltage waveforms and a.c. losses has been studied in a previous paper (part I) [5].

In the literature, various methods have been presented for the experimental determination of the critical current density j_c and its dependence on magnetic induction, $j_c(B)$, or position, $j_c(x)$ [1]. With respect to the surface currents, however, only a measure for irreversibility of these currents has been obtained so far by measuring the maximum a.c. field amplitude which does not give rise to flux penetration in the bulk of the sample [6]. In a previous paper [3], the authors have presented an inductive technique making use of trapezoidal a.c. fields with which the complete $B_{en}(B_a)$ and $B_{ex}(B_a)$ curves can be determined experimentally. The technique also allows the measurement of $j_c(x)$. In the present work this technique will be used to determine the superconducting properties of a Nb–50% Ti alloy. Both the $j_c(x)$ relation as well as the $B_{en}(B_a)$ relation have been determined and compared with results obtained with other techniques. For an additional check, the experimental relations have been introduced in the numerical model calculations [5]. In this way both the possibilities and the limitations of the technique have been demonstrated.

A short description of the experimental technique will be given in section 2. After that the experimental results will be presented in section 3. Here the shape of the induced voltage waveforms will be discussed followed by an analysis of the flux distribution, j_c-values and $B_{en}(B_a)$ and $B_{ex}(B_a)$ relations. The results of a.c. loss measurements have already been published elsewhere [5, 7]. In section 4 the experimental voltage waveforms will be compared with calculated curves. Finally, in section 5 conclusions with respect to the experimental technique will be drawn.

0378-4363/82/0000–0000/$02.75

2. Experimental technique

In order to separate the contributions of bulk and surface currents, the superconducting slab (thickness $2d$) has been subjected to a trapezoidal a.c. magnetic field (amplitude b_0) superposed on a static field B_0. The complete waveform of the voltage induced in a pick-up coil has been recorded and analyzed. A detailed description of the technique has already been given elsewhere together with a description of the experimental equipment [3, 4]; here we will restrict ourselves to the main characteristics. The method is based on the validity of the C.S.M. and starts from the following assumptions:

(1) Flux flow effects may be neglected.

(2) The influence of $\partial j_c/\partial B$ may be neglected.

Under these conditions the induced voltage $E(t)$ in increasing field can be written as

$$E(t) = (d - x_t)\frac{dB_{en}}{dB_a}\frac{dB_a}{dt}, \tag{1}$$

where x_t is the position of the flux front, i.e. the position to which the flux change has penetrated. As a consequence of the trapezoidal waveform of the a.c. field, dB_a/dt is constant. When the flux front has reached the central plane of the slab ($x_t = 0$), the induced voltage becomes independent of the starting value of the a.c. field. This means that all induced voltage waveforms measured with the same amplitude of the a.c. field but with different static fields B_0, approach the same envelope curve $E_1(B_a)$, which is proportional to dB_{en}/dB_a. It may now be deduced from eq. (1) that

$$\frac{E}{E_1} = \frac{d - x_t}{d}, \tag{2}$$

which gives the position of the flux front. The corresponding B-value can be obtained from

$$B(x_t, B_a) = B_{ex}(B_0 - b_0) + \frac{1}{2}\int_{B^+_{a_0}}^{B_a} \frac{dB_{en}}{dB_a}\, dB_a, \tag{3}$$

where $B^+_{a_0}$ is the external field value at which flux starts to penetrate the bulk of the sample.

Where dB_{en}/dB_a is constant the flux distribution may be determined simply by turning the E vs. B_a curve over 90 degrees; otherwise some additional calculations according to (2) and (3) are necessary. In both cases the line $E = 0$ may be considered as the surface of the slab while the envelope curve E_1 gives the central plane.

The amount of flux ΔB_p screened by the bulk of the sample is obtained by integration of the flux distribution. This value is related to B_{en} (B_a) and the average flux density B_{av} according to

$$B_{av} = B_{en}(B_a) - \Delta B_p. \tag{4}$$

By repeating the experiment at a large number of B_0-values, B_{av} can be determined [3] and the value of $B_{en}(B_a)$ follows from (4). In an analogous way the $B_{ex}(B_a)$ curve can be obtained.

The main reason for errors in this procedure is that for many materials $\partial j_c/\partial B$ may not be neglected, especially around $B = 0$. An estimate of the relative error ϵ in the flux distributions, based on simple analytical arguments and numerical model calculations leads to

$$\epsilon > \mu_0 d \left.\frac{\partial j_c}{\partial B}\right|_{B_0 - b_0}. \tag{5}$$

As can be seen from (4) this is also the main error in $B_{en}(B_a)$. The actual value of these errors strongly depends on the properties of the material under consideration. The validity of the method has been verified by means of numerical model calculations [3].

3. Experimental results

3.1. Sample description

The experiments have been performed on Nb–50% Ti slab, manufactured from powders by

means of electron gun melting in a vacuum of 10^{-8} Torr. After that it was cut to its final dimensions ($20 \times 5 \times 0.3\ mm^3$) and polished mechanically. Its behaviour is characterized mainly by a bulk critical current density j_c. In the frequency range used in these experiments ($dB_a/dt \leq 15$ T/s) flux flow effect may be neglected; this has been concluded from the steep decay in E at those corners of the trapezium where the applied field variation has stopped. Experimental values of the resistivity of Nb–65% Ti [8] at 11 K lead to a time constant of 30 ns which is far beyond the reach of our equipment. Surface screening effects play a role only in the low-field region; as will be seen later the field of first penetration is approximately 14 mT. In the C.S.M. the behaviour under quasi-static conditions can be described in terms of a $j_c(B, x)$ relation together with $B_{en}(B_a)$ and $B_{ex}(B_a)$. For the determination of these three relations, experiments with different a.c. field amplitudes ($b_0 = 180$, 61, 30 and 15 mT) in a large range of static fields ($0 \leq B_0 \leq 1.6$ T) have been performed. The shape of the induced voltage curves will be discussed in section 3.2. The flux distribution and the j_c-values derived from these curves will be presented in section 3.3 and the $B_{en}(B_a)$ and $B_{ex}(B_a)$ curves in section 3.4.

3.2 Induced voltage curves

A series of E vs. B_a curves for various static fields is shown in fig. 1. As expected, the plots for increasing and decreasing fields are images of each others with respect to $B_a = 0$. The general behaviour is in qualitative agreement with the calculated curves presented in part I. When the external field is increased from a very high negative value, the induced voltage (the envelope curve) decreases from its original value 1 to approximately 0.3 at a value of B_a slightly above $B_a = 0$. After that, a sharp increase of E occurs, followed by a double maximum and a decrease to 1 at high B_a-values. This behaviour has been discussed in section 3 of part I. The occurrence of a double maximum may be explained by the presence of surface screening currents (compare with fig. 3 of part I). An interval with $E = 0$ has not been observed; from this it has been concluded that no intervals in which B_{en} or B_{ex} equals zero occur in the $B_{en}(B_a)$ and $B_{ex}(B_a)$ curves. When the external field is increased from the minimum value $B_a = B_0 - b_0$, the induced voltage gradually increases until the envelope curve has been reached. From this moment, flux changes occur all over the sample and during a further increase of B_a, E follows the envelope curve. It may be mentioned here that due to the large value of B_{c_2} for Nb–Ti alloys, it has not been possible to use the normal state response E_n for the normalization of E [3]. As a good approximation the value of the envelope curve at a high static field ($B_0 = 1.6$ T) has been used for E_n.

Some induced voltage curves with static fields in the range $270 < B_0 < 380$ mT are shown in fig. 2a as a function of the total external field B_a. The envelope curve is constant in this region. The same curves are also shown in fig. 2b, but as a function of the a.c. component of B_a only. In this case the flux distribution inside the slab can be obtained by turning the E/E_n vs. B_a plot over 90 degrees. Now, the $E/E_n = 0$ axis indicates the surface of the conductor while the envelope curve indicates the central plane of the slab. A more detailed discussion of the shape of these flux distributions near the surface will be given in the next section.

A very remarkable behaviour can be observed when E approaches the envelope curve. In contrast to the calculated curves where a sharp transition to the envelope curve (a kink) has been found, a rather smooth transition has been observed experimentally. In terms of flux distributions this suggests a considerable increase of j_c near the centre of the sample, which is very unlikely. A similar behaviour has also been observed in a Nb-slab [2]. This effect may be explained by an inhomogeneous distribution of pinning sites in the bulk of the sample: j_c depends on the y and z coordinates. As a result

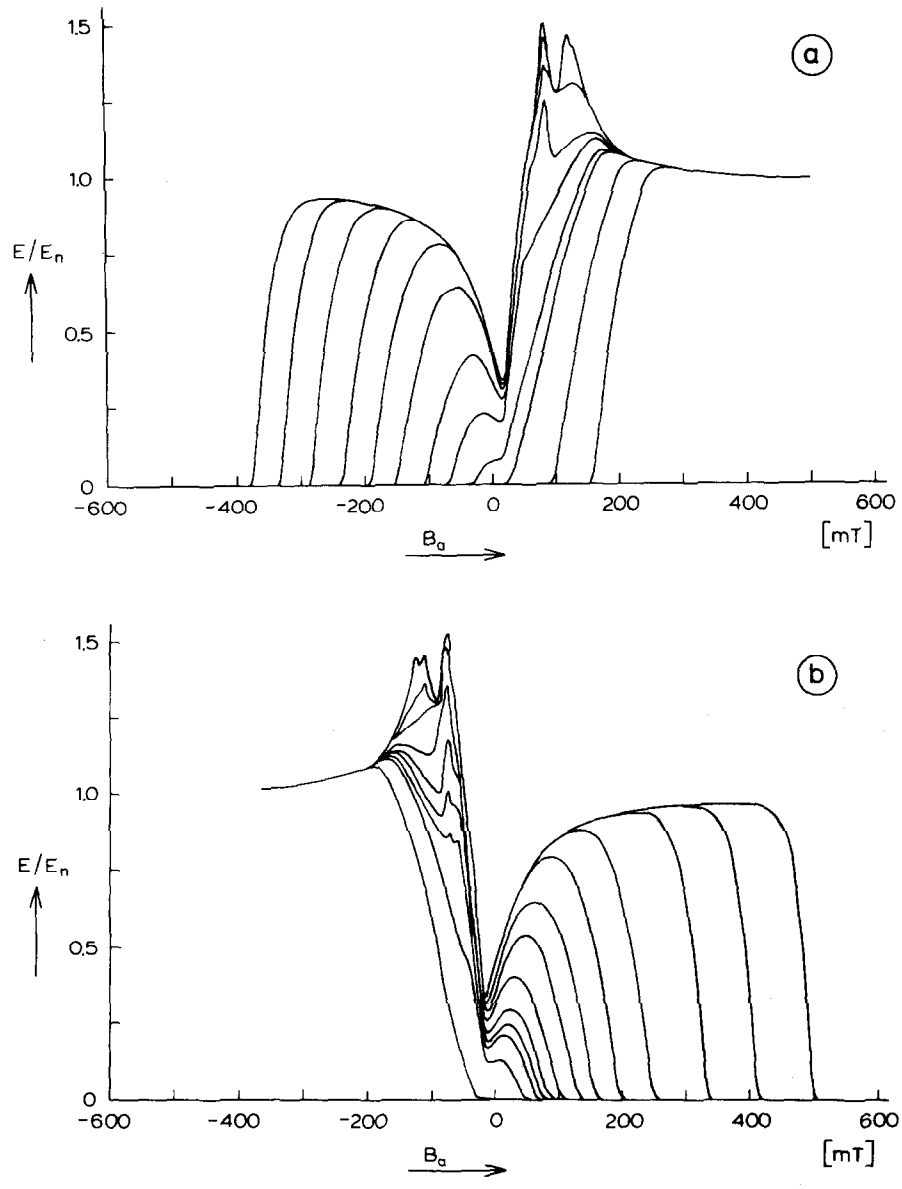

Fig. 1. Induced voltage curves in increasing (a) and decreasing field (b) for Nb–50% Ti and various values of the static field $B_0(-200 < B_0 < 300$ mT; $b_0 \approx 180$ mT; $dB_a/dt = 14.9$ T/s).

the flux front is not a flat surface and x_t has to be defined as an average value. Near the central plane where the two flux fronts of the two halves of the slab meet, the determination of x_t from E/E_1 is no longer valid because at one position the two flux fronts meet at a different B_a-value than at another position. This leads to a smooth transition to the envelope curve. In this region the determination of the flux distribution according to (2) and (3) breaks down. Analogous considerations hold for inhomogeneous surface screening and surface roughness.

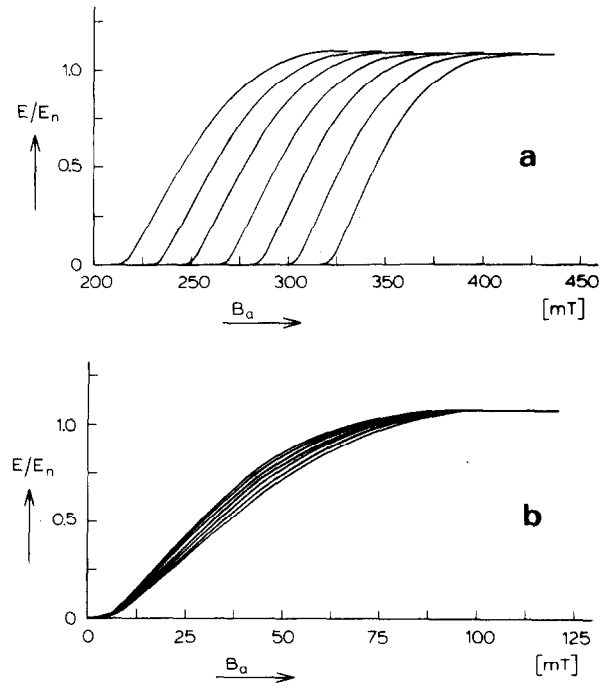

Fig. 2. The induced voltage for various values of B_0 ($270 < B_0 < 380$ mT; $b_0 \approx 61$ mT; $dB_a/dt = 14.7$ T/s) plotted versus (a) total field and (b) a.c. field only.

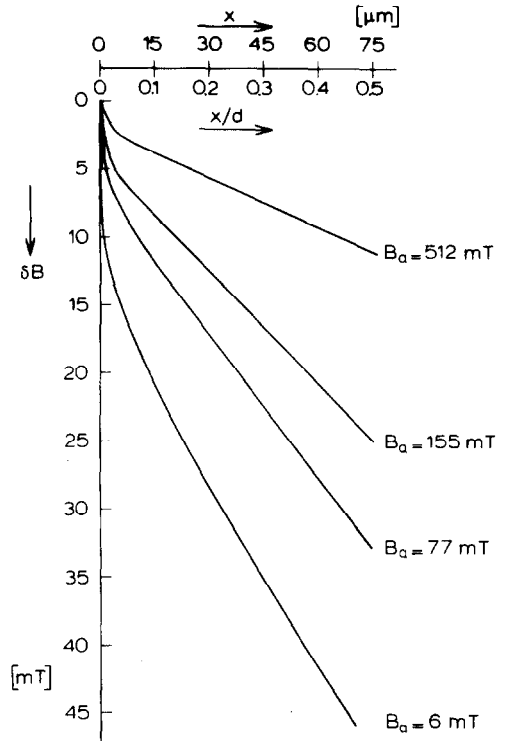

Fig. 3. Flux distribution in a Nb–50% Ti slab for various values of the external field (d is half the thickness of the slab: $d = 0.15$ mm).

3.3. Flux distributions and critical current densities

From the induced voltage curves flux distributations have been determined according to eqs. (2) and (3). Some of these flux distributions are shown in fig. 3. Only the distribution near the surface has been given; the central area of the slab has been omitted because of the deviations in this region caused by inhomogeneities. In the profiles three different regions can be distinguished.

First of all, at low fields, surface screening currents in a very narrow layer near the surface can be observed. The thickness of this layer cannot be estimated from the measurements. Secondly, near the surface a small layer with a thickness of approximately $3\,\mu$m with a relatively high critical current density ($j_c \approx 0.8 \times 10^5$ A cm^{-2} at $B_a = 150$ mT) can be distinguished. The fact that the thickness of this layer is independent of frequency and magnetic induction shows that the behaviour in this region may indead be attributed to enhanced pinning and not to inhomogeneous surface screening or flux flow. Finally, in the bulk of the sample a constant j_c can be observed.

Values of the critical current density in the bulk of the sample have been determined from the gradient of the flux distribution by means of a least-square deviation fit. The results are shown in fig. 4 in the field range between $0.1 < B_a < 1.6$ T. Experiments with three different amplitudes have been used, as well as the results obtained from the increasing and the decreasing parts of the trapezoidal a.c. field. The results agree well. The values obtained here are about a factor 10 lower compared with the values reported in the literature [9]. The values of j_c obtained from the same sample by means of a d.c. mag-

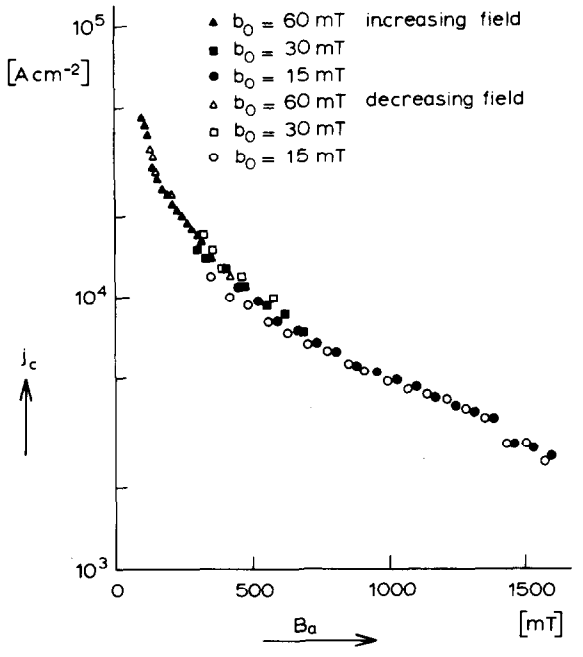

Fig. 4. Critical current density of Nb–50% Ti as a function of external field. The values have been obtained with a.c. fields of three different amplitudes and from the increasing as well as decreasing part of the a.c. field.

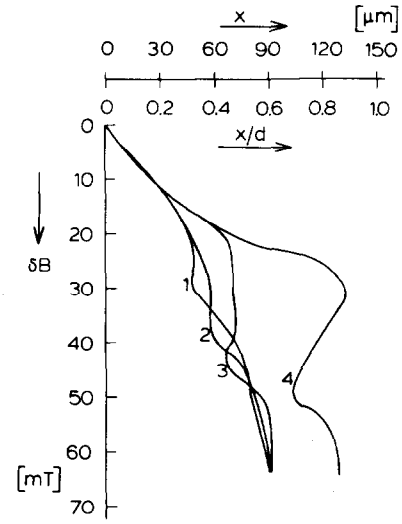

Fig. 5. "Flux distributions" obtained according to eqs. (2) and (3) at low fields (1; B_a = 17 mT; 2: B_a = 34 mT; 3: B_a = 52 mT; B_a = 67 mT). The strange shape is not realistic – the result of large errors around $B = 0$.

netization [10] are somewhat lower than the results from experiments with trapezoidal a.c. fields. A similar discrepancy has been observed by Kroeger et al. [11] in a Nb–25% Ti sample.

An estimate of the error according to eq. (5) leads to $\epsilon \approx 15\%$ at $B_a = 0.1$ T and $\epsilon < 2\%$ for $B_a > 0.5$ T. In the low-field region ($B_a < 0.1$ T) no satisfactory results have been obtained. Some "flux distributions" in this region are shown in fig. 5. The curves exhibit a strange bump which may be attributed to the large variations of j_c. This means that the main conditions of the method are not met and therefore the flux profiles are not correct. The j_c-values determined in this region are much too high as can be seen in fig. 6 where the j_c-values in the low-field region versus magnetic induction have been plotted. An extrapolation of the results for $|B_a| < 100$ mT has also been indicated.

3.4. $B_{en}(B_a)$ and $B_{ex}(B_a)$ relations

The values of B_{en} and B_{ex} for various values of B_a have been determined according to eq. (4). The amount of flux screened by bulk currents ΔB_p has been determined by a numerical integration of the whole flux distribution including the region near the central plane. The latter region, in which a smooth transition to the envelope curve occurs, has to be taken into account because all bulk currents have to be considered. The full bulk screening has been reached when the flux fronts have met completely. Numerical integration also takes into account the enhanced pinning layer near the surface. The B_{av} vs. B_a envelope curves have been determined from a large number of small hysteresis loops. The values of B_{en} and B_{ex} obtained in this way are shown in fig. 7. the maximum amplitude b_0 for which no flux change penetrates to the bulk of the sample can be determined from these curves according to $b_0 = \frac{1}{2}(B_1 - B_2)$ with $B_{en}(B_1) = B_{ex}(B_2)$. The values obtained in this way, which are shown in fig. 8,

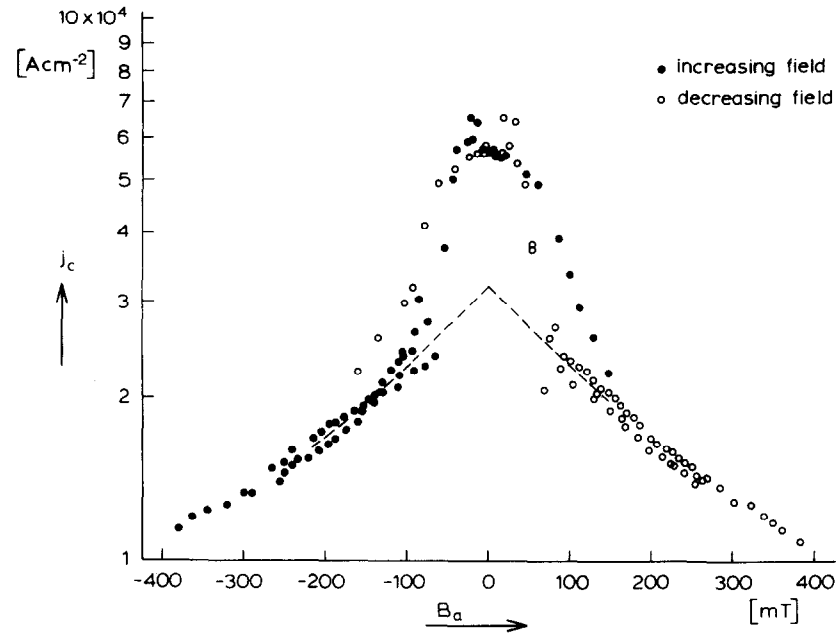

Fig. 6. Critical current density as a function of B_a in the low field region; the values have been determined with an a.c. field as in fig. 1. Around $B_a = 0$ no realistic results have been obtained.

are in agreement with the results of a direct measurement of this amplitude [10].

The $B_{en}(B_a)$ and $B_{ex}(B_a)$ curves shown in fig. 7 are not in agreement with the theoretical curves, predicted by Clem [12] which can be written as

$$B_{en}(B_a) = (B_a^2 - B_s^2)^{1/2}, \tag{6a}$$

$$B_{ex}(B_a) = B_a. \tag{6b}$$

The relations proposed by Ternowskii et al. [13] also do not apply. A model for more realistic relations has been given elsewhere [4, 14]. In this model the deviation of the experimental $B_{en}(B_a)$ relation from eq. (6a) is ascribed to inhomogeneities in the surface screening caused by demagnetization effects due to surface roughness. A similar model for the discrepancy between the experimental $B_{ex}(B_a)$ curve and (6b) does not apply since (6b) does not lead to any demagnetization effects. Therefore, it has to be concluded that relation (6b) does not apply for Nb–50% Ti, even in the ideal case.

4. Comparison with calculated results

A comparison of the waveform of the induced voltage with the calculated E vs. B_a curves (see part I) shows a good qualitative agreement. It can be seen that the overall behaviour is a consequence of the variation of $j_c(B)$ but the double peak in the induced voltage is caused by surface screening. As an additional confirmation of the measuring technique, the experimental $j_c(B)$, $B_{en}(B_a)$ and $B_{ex}(B_a)$ relations have been used in the model calculations. The $j_c(B)$ relation has been approximated by

$$j_c(B) = j_c(0)/(1 + |B|/B_1), \tag{7}$$

with $j_c(0) = 0.4 \times 10^5$ A cm^{-2} and $B_1 = 80$ mT. Since no functional dependence is known to describe the $B_{en}(B_a)$ and $B_{ex}(B_a)$ curves, these relations have been expressed in the form of two discrete arrays of numbers which have been taken from the experiments. As a consequence, the calculated E vs. B_a curve, which is shown in

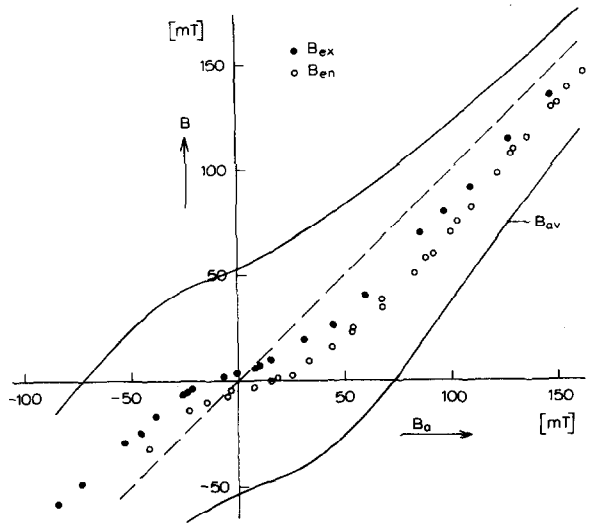

Fig. 7. $B_{en}(B_a)$ and $B_{ex}(B_a)$ curves for Nb–50 Ti. The points have been obtained according to eq. (4) from experiments with amplitude $b_0 = 180$ mT $(-300 < B_0 < < +300$ mT, $dB_a/dt = 14.9$ T/s). The envelope curve $B_{av}(B_a)$ is also shown.

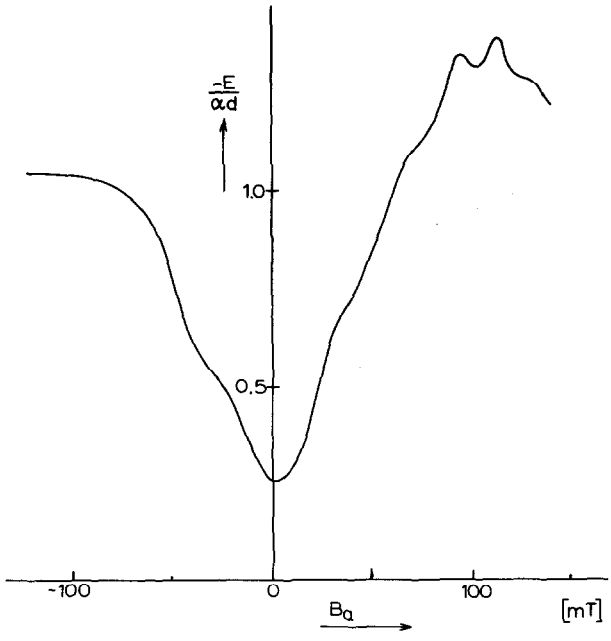

Fig. 9. The calculated E vs. B_a curve using the results of figs. 4 and 7.

fig. 9 exhibits some bumps which have to be attributed to irregularities in the $B_{en}(B_a)$ and $B_{ex}(B_a)$ curves. In general the correspondence between the calculated and measured curves is quite good. Therefore, it may be concluded that the behaviour of the Nb–50% Ti slab can indeed be described in terms of the $j_c(B)$, $B_{en}(B_a)$ and $B_{ex}(B_a)$ relations as determined from experiments with trapezoidal a.c. fields. This conclusion is supported by the results of the a.c. loss measurements presented in part I. There it has been found that some features of the a.c. loss as a function of d.c. bias field can be explained only when the $B_{en}(B_a)$ and $B_{ex}(B_a)$ relations in section 3.4 are taken into account.

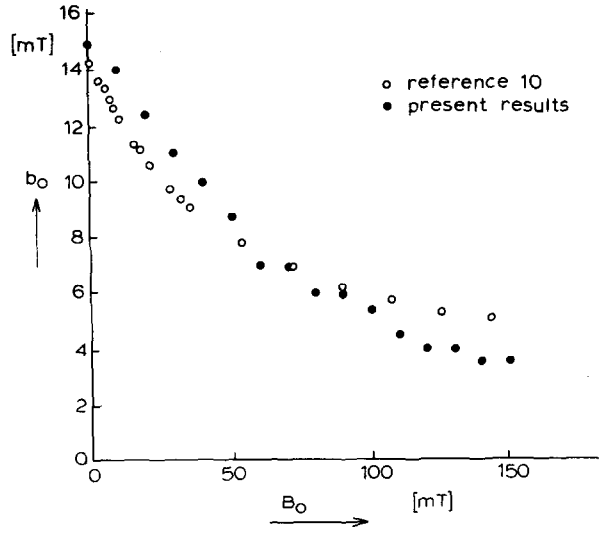

Fig. 8. The maximum amplitude b_0 for which no flux change penetrates to the bulk versus the value of the static field.

5. Conclusions

It has been shown in this paper that the behaviour of Nb–50% Ti can be explained in terms of the quasi-static critical state model with a critical current density j_c which depends on B and x and with surface screening currents described by $B_{en}(B_a)$ and $B_{ex}(B_a)$ relations. These parameters have been determined experimentally. For this purpose an inductive technique

based on the direct observation of the complete induced waveform due to a trapezoidally varying a.c. field [3, 4] of sufficiently large amplitude has been used. With this technique the flux distribution inside the sample has been determined as a function of magnetic induction, or, in other words, the dependence of j_c on magnetic induction and distance to the surface. By combining these results with the B_{av}–B_a curve the $B_{en}(B_a)$ and $B_{ex}(B_a)$ curves which describe the actual value of the surface currents has been determined.

The correctness of the results on Nb–50% Ti has been demonstrated by the good qualitative and quantitative agreement between the experimental induced voltage waveform and curves calculated numerically with the help of the obtained $j_c(B)$, $B_{en}(B_a)$ and $B_{ex}(B_a)$ relations. Moreover, the results correspond well with the values measured with alternative techniques. It has not been possible to determine flux distributions in the whole B-range. This is caused by the fact that for small B-values ($B < 100$ mT) one of the main assumptions on which the method is based is not satisfied. In this range the dependence of j_c on magnetic induction is too strong. Another basic assumption of the method has been sufficiently satisfied; flux flow effects may be neglected. It may be noted here that when this is not the case, the flux flow conductivity σ_{ff} can also be determined from experiments with trapezoidal a.c. fields as has been demonstrated elsewhere [15].

Acknowledgements

The authors are indebted to Mr. M. Ciszek for his kind disposal of the sample and his assistance during the measurements. Also the cooperation of Mr. J. Sikkenga in the numerical evaluation is gratefully acknowledged.

References

[1] A.M. Campbell and J.E. Evetts, Adv. in Phys. 21 (1972) 199.
[2] L.J.M. van de Klundert, E.A. Gijsbertse and H.P. van der Braak, Physica 94B (1978) 41.
[3] E.A. Gijsbertse, M. Caspari and L.J.M. van de Klundert, Cryogenics (1981) 299.
[4] E.A. Gijsbertse, Thesis, Enschede (October, 1980).
[5] E.A. Gijsbertse, J. Sikkenga and L.J.M. van de Klundert, Physica 106B (1981) 59.
[6] H. Ullmaier, Phys. Stat. Sol. 17 (1966) 631.
[7] M. Ciszek, G. Kozlowski, P. Tekiel, E.A. Gijsbertse and L.J.M. van de Klundert, Phys. Lett. 77A (1980) 271.
[8] A.D. McInturff, in Metallurgy of Superconducting Materials, T. Luhman and D. Dew Hughes, eds. (Academic Press, New York, 1979) p. 109.
[9] See ref. [8], p. 99–120.
[10] M. Ciszek and G. Kozlowski, private communications.
[11] D.M. Kroeger, C.C. Koch and J.P. Charlesworth, J. Low. Temp. Phys. 19 (1975) 493.
[12] J.R. Clem, Proc. LT 13, Vol. 3 (Plenum, New York, 1974) p. 102.
[13] F.F. Ternowskii and L.N. Shekhata, Sov. Phys. JEPT 35 (1972) 1202.
[14] E.A. Gijsbertse and L.J.M. van de Klundert, Phys. Lett. 82A (1981) 188.
[15] E.A. Gijsbertse and L.J.M. van de Klundert, Physica 103B (1981) 315.